AFRL-RZ-WP-TP-2011-2060

IMPROVED SIMULATION OF INFLOW DISTORTION FOR DIRECT-CONNECT SCRAMJET STUDIES

Hagenmaier, Mark A.
Propulsion Sciences Branch (AFRL-RZAS)
Aerospace Propulsion Division

Eklund, Dean R.
Propulsion Sciences Branch (AFRL-RZAT)
Aerospace Propulsion Division

INTERIM
APRIL 2011

Approved for public release; distribution unlimited.

STINFO COPY

AIR FORCE RESEARCH LABORATORY
PROPULSION DIRECTORATE
WRIGHT-PATTERSONAIR FORCE BASE, OH 45433-7251
AIR FORCE MATERIEL COMMAND
UNITED STATES AIR FORCE

REPORT DOCUMENTATION PAGE

Form Approved
OMB No. 0704-0188

1. REPORT DATE *(DD-MM-YYYY)*	2. REPORT TYPE	3. DATES COVERED *(From - To)*
April 2011	**Interim Report**	**May 2010 – Apr 2011**

4. TITLE AND SUBTITLE

Improved Simulation of Inflow Distortion for Direct-Connect Scramjet Studies

5a. CONTRACT NUMBER
In-House

5b. GRANT NUMBER

5c. PROGRAM ELEMENT NUMBER
61102F

6. AUTHOR(S)

Mark A. Hagenmaier; Ryan T. Milligan
Dean R. Eklund

5d. PROJECT NUMBER
2308

5e. TASK NUMBER
AI

5f. WORK UNIT NUMBER
2308AI02

7. PERFORMING ORGANIZATION NAME(S) AND ADDRESS(ES)

Propulsion Sciences Branch (AFRL/RZAS)
Aerospace Propulsion Division

8. PERFORMING ORGANIZATION REPORT

9. SPONSORING / MONITORING AGENCY NAME(S) AND ADDRESS(ES)

Air Force Research Laboratory
Propulsion Directorate
Wright-Patterson AFB, OH 45433-7251
Air Force Materiel Command
United States Air Force

10. SPONSOR/MONITOR'S ACRONYM(S)

AFRL/RZAS

11. SPONSOR/MONITOR'S REPORT NUMBER(S)

AFRL-RZ-WP-TP-2011-2060

12. DISTRIBUTION / AVAILABILITY STATEMENT

Approved for public release; distribution unlimited. Date Cleared: 17 December 2010; PA Case No: 88ABW-2010-6580

13. SUPPLEMENTARY NOTES

This document contains color.

14. ABSTRACT

A technique to develop flight-like inflow conditions for direct-connect testing has been extended in the current work. This technique utilizes an expansion/contraction section upstream of the engine isolator in a direct-connect test facility to create shock waves consistent with those generated in flight. The current work improves upon the earlier work by better matching the inlet shock structures, the average conditions at the engine throat, and boundary layer properties. RANS CFD simulations have been performed for isolators downstream of a flight inlet, a direct-connect facility nozzle without distortion, and a direct-connect facility nozzle with distortion. The RANS CFD simulations predict similar shock positions in all cases, however a change in the mass flux distribution at the exit plane is observed.

15. SUBJECT TERMS:
Computational Fluid Dynamics, SCRAMJET

16. SECURITY CLASSIFICATION OF:			17. LIMITATION OF ABSTRACT	18. NUMBER OF PAGES	19a. NAME OF RESPONSIBLE PERSON
a. REPORT	b. ABSTRACT	c. THIS PAGE			**Mark A. Hagenmaier**
Unclassified	**Unclassified**	**Unclassified**	**SAR**	**16**	19b. TELEPHONE NUMBER *(include area code)* **937-255-7325**

Standard Form 298 (Rev. 8-98)
Prescribed by ANSI Std. 239.18

Table of Contents

List of Figures

List of Tables

List of Equations

List of Nomenclature

S:	streamwise distance from the start of the shock train
H:	isolator duct height
Θ:	momentum thickness at the start of the shock train
Re_θ:	Reynolds number based on momentum thickness
M_1:	(average) Mach number at the start of the shock train
P:	(average) static pressure
p_1:	(average) static pressure at the start of the shock train
x:	streamwise distance from start of isolator
y:	normal distance from body

1.0 Summary

A technique to develop flight-like inflow conditions for direct-connect testing has been extended in the current work. This technique utilizes an expansion/contraction section upstream of the engine isolator in a direct-connect test facility to create shock waves consistent with those generated in flight. The current work improves upon the earlier work by better matching the inlet shock structures, the average conditions at the engine throat, and boundary layer properties. RANS CFD simulations have been performed for isolators downstream of a flight inlet, a direct-connect facility nozzle without distortion and a direct-connect facility nozzle with distortion. The RANS CFD simulations predict similar shock positions in all cases, however a change in the mass flux distribution at the exit plane is observed.

2.0 Introduction

Development of supersonic combustion ramjet (scramjet) engines commonly involves several phases of experimental evaluation in close collaboration with computational fluid dynamics (CFD) simulations. Generally, component-level experiments are conducted in freejet (for inlet-isolator components) and direct-connect (for isolator-combustor components) facilities, while the integrated engine (inlet-isolator-combustor-nozzle) is evaluated in a freejet or semi-freejet facility prior to flight testing.

In the direct-connect test environment, scramjet combustor simulations are typically accomplished using a facility nozzle that is designed to produce a uniform, supersonic gas stream with one-dimensionally averaged flow properties that match the expected conditions at the engine throat (entrance to the engine isolator) in a flight vehicle. While this test environment offers substantial advantages over the freejet environment (reduced experimental complexity, potentially longer test duration, generally simplified test article design constraints, more flexible instrumentation options, etc.), direct-connect testing does not reproduce the highly distorted flow profile caused by oblique shocks generated in the scramjet inlet. This raises concerns that the performance and operability results obtained in direct-connect experiments may not be representative of the freejet and/or flight environments. Another consideration is that freejet testing of large scramjets (e.g. for space access) is not possible in existing ground test facilities. Development of these large scale scramjets will likely proceed directly from direct-connect testing to flight. In that case, it may be critical to simulate the inlet distortion in the direct-connect testing as is done in turbojet engine development.

In prior work[1], a method to simulate this distortion in a direct-connect scramjet test facility was demonstrated. The approach used was a non-traditional form of direct-connect testing, where a facility nozzle was used to generate the average conditions at a plane upstream of the engine throat where the conditions in the full engine are nearly uniform. Starting at this plane, the full engine geometry was replicated, causing the shocks generated within the direct-connect hardware to be consistent with those in the full engine. The hardware that was built to test this distortion generation approach was used for numerous combustor studies; however, a thorough comparison of the engine performance with and without flow distortion was not completed due to unexplained flow non-uniformities in the non-distorted case.

The present work is part of a larger effort to study scramjet flow phenomena. In the current work, CFD is used in the design of a direct-connect device that will generate flow distortion consistent with flight. As will be shown, the distortion generation device provides an excellent match of the shock structure and the mean flow quantities of the flight inlet. In later work, the isolator flowfield for un-distorted and distorted inflows will be studied in an optically accessible isolator section.

It is important to note that in both traditional and non-traditional direct-connect testing, the boundary layer characteristics may not adequately match those that exist in the full engine. Boundary layer modification (e.g., bleed, mass injection, or vortex generators) may be used to improve the match; a limited investigation of these approaches is explored in the current work.

3.0 Methods

Reynolds-averaged Navier Stokes (RANS) computational fluid dynamic (CFD) calculations have been performed with CFD++ from Metacomp Technologies[2]. The code has a finite-volume numerical framework with Riemann solvers for accurate representation of supersonic flows. Shock discontinuities were handled using the HLLC Riemann solver with a continuous flux limiter. The realizable k-ε turbulence model was used to represent the

apparent turbulent stresses. The realizability criterion accounts for known physical properties of the stress tensor by bounding the magnitude of the tensor components, which improves accuracy and stability. Multi-grid acceleration was used to provide accelerated convergence for steady flows.

Structured grids for all configurations were generated with Gridgen from Pointwise[3]. The grids for the flight inlet, direct-connect nozzles and distortion generation hardware used a wall spacing for solve-to-wall turbulence models (i.e. y+ near 1), and spacing in the core flow of approximately 1 mm. The grids for the isolator used a wall spacing for a wall-function turbulence model (i.e. y+ near 20), and spacing in the core flow of approximately 1 mm.

To represent spatially averaged quantities at a streamwise station, the separated flow averaging procedure[4,5] was used. This "average" adds two distortion terms to represent the flow as a separated flow, a core flow with a stagnant region. This averaging technique preserves conserved flow quantities (mass flow, stream thrust, energy flow), and closely maintains the true entropy of the flow without large deviations in static pressure and temperature.

4.0 Discussion of Results

4.1 Development of Direct-Connect Distortion Generation Hardware

Prior work[1] aimed to develop representative distortion for the AFRL/RZA direct-connect combustor hardware in Research Cell 22 (RC22), with 42.4 mm high and 228.6 mm wide cross-section, and a throat Mach number of approximately 2.5. That study focused on understanding the performance impacts of the flow distortion on isolator performance. RC22 had limited capabilities for optical diagnostics, and was unable to support a more fundamental study of the impact of flow distortion.

The present work applies a similar approach to create a representative distortion for AFRL/RZA direct-connect combustor hardware in Research Cell 18 (RC18), which has the capability to support advanced optical diagnostics in the isolator section. The cross-section of RC18 is 38.1 mm x 101.6 mm, and a facility nozzle exists which provides uniform flow with a throat Mach number of approximately 2.18.

Figure 1 shows a diagram of the flow structure in a planar compression inlet. An expansion fan is generated by the turning of the body wall at the throat (called the shoulder), but has been excluded in this diagram. In each of the flow regions upstream of the engine throat (noted as 0, A, B, and C in the figure) the flow properties are nearly constant. In a traditional direct-connect study, a facility nozzle is used which matches the average condition at the engine throat (noted as "throat" in the figure).

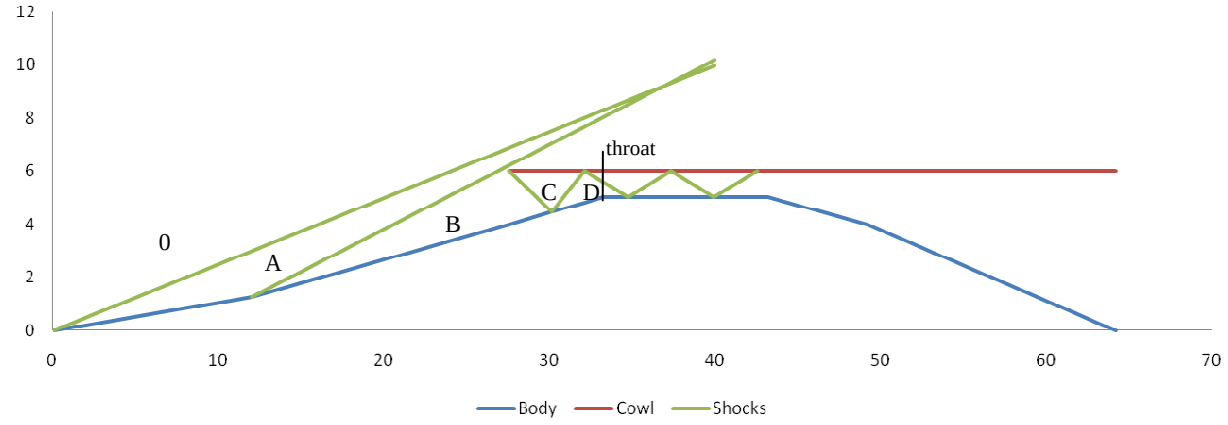

Figure 1: Planar compression scramjet flow structure

One empirical model for isolator performance[6] in rectangular ducts is expressed as:

$$\frac{(M_1^2 - 1)\left(\frac{S}{H}\right)\mathrm{Re}_\theta^{0.2}}{\sqrt{\theta/H}} = 50\left(\frac{p}{p_1} - 1\right) + 170\left(\frac{p}{p_1} - 1\right)^2$$

Equation 1: Rectangular duct isolator model from Sullins, et. al.

This shows that isolator pressure rise is dominated by the incoming Mach number M_1, and the momentum thickness θ. Therefore, matching the average Mach number and the momentum thickness is a goal in the development of the distortion generator.

To understand the impact of flow distortion on isolator performance, it is desired to compare a full engine, a direct-connect engine without inflow distortion (i.e. the traditional approach), and a direct-connect engine with inflow distortion. All three testing modes are investigated in the current study using RANS CFD modeling tools, and the two direct-connect modes will be studied in a future experimental study in RC18.

4.1.1 Flight Mode

A generic inlet is considered for this study, which employs a single 6 degree forebody turning angle, and a cowl that turns the flow back to the axial direction. This is obviously not an optimized inlet, but the cowl turning angle, which dictates the strength of the internal shocks that create the flow distortion, is representative of planar compression scramjets. The Mach number and angle of attack of the flight inlet were varied such that the average Mach number at the throat was 2.18, to be consistent with an existing facility nozzle available for RC18. For the present study, a flight condition of Mach 4, dynamic pressure of 95.7 kPa (2000 psf), and an angle of attack of 9.2 degrees provided the desired throat Mach number of 2.18.

Figure 2(a) shows the Mach distribution on the center plane, while the Figure 3 shows the average Mach for each streamwise location. Figure 4 (a) shows the pressure distribution on the centerplane, while Figure 5 shows the average pressure for each streamwise location.

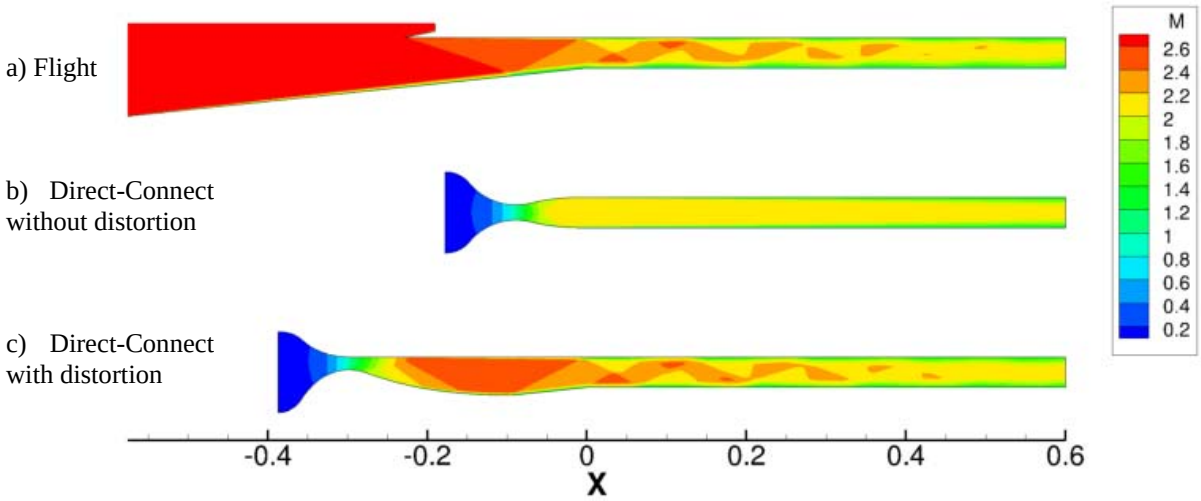

Figure 2: Center plane Mach for flight and direct-connect conditions

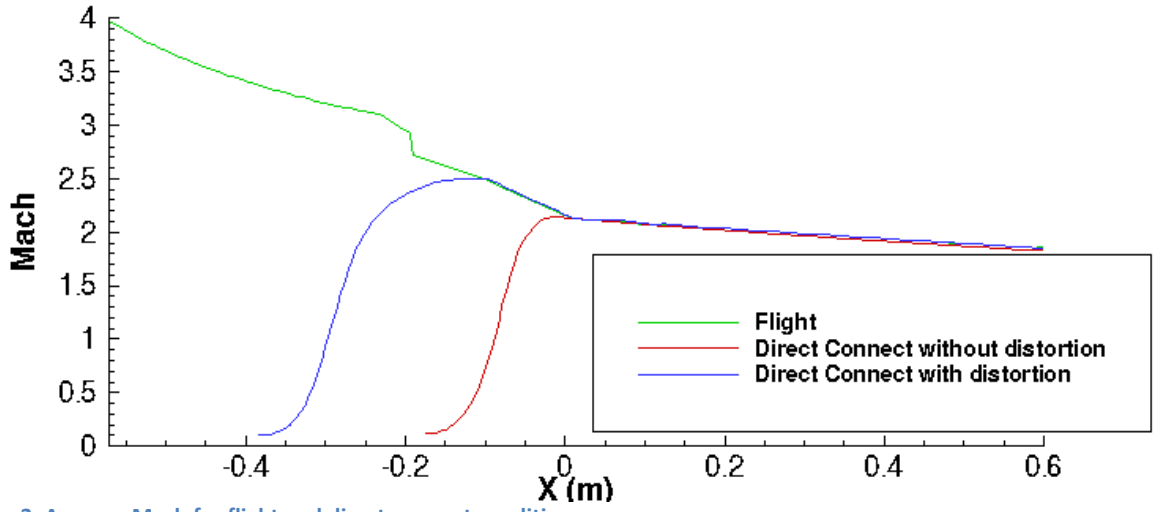

Figure 3: Average Mach for flight and direct-connect conditions

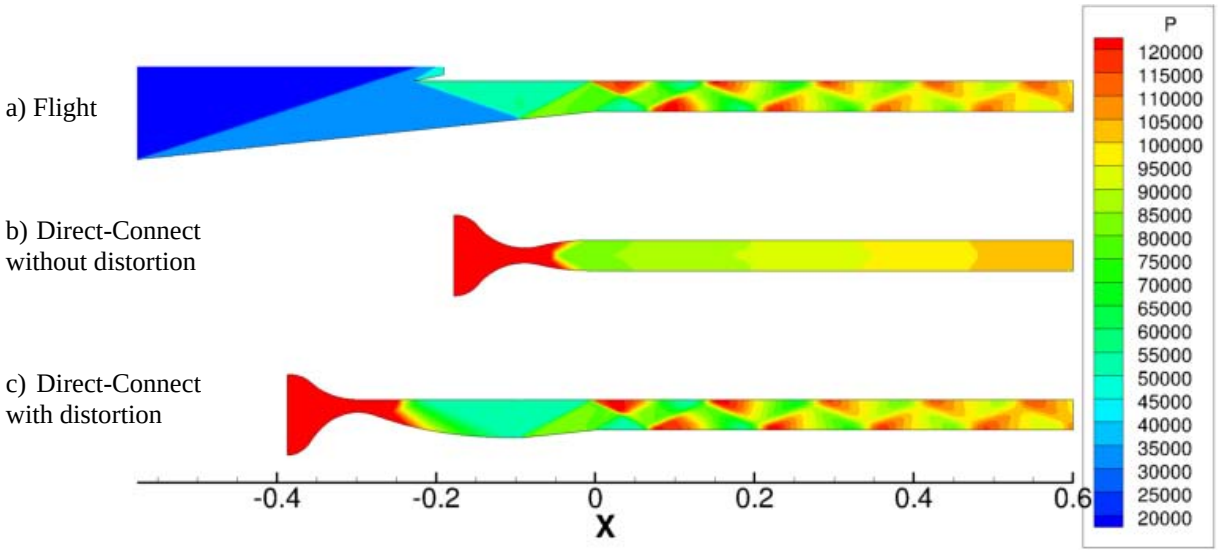

Figure 4: Center plane pressure for flight and direct-connect conditions

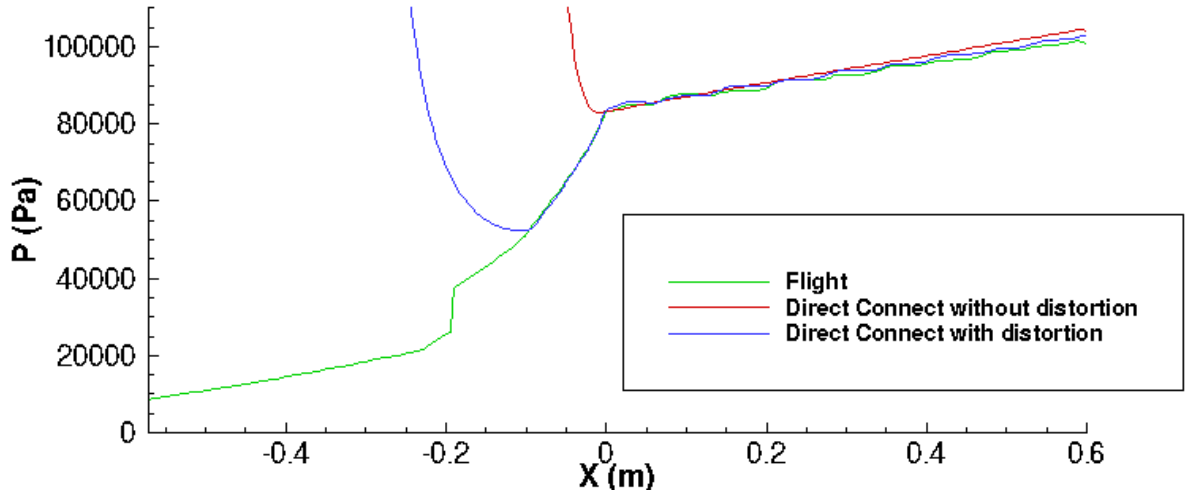

Figure 5: Average pressure for flight and direct-connect conditions

4.1.2 Non-distorted direct-connect mode

An existing RC18 facility nozzle, which produces near-uniform flow, was analyzed for consistency with the flight inlet. The nozzle area ratio is approximately 2.0. At conditions consistent with Mach 4 flight at a dynamic pressure of 95.7 kPa (2000 psf), the average Mach number at the engine throat is 2.18. This throat condition is consistent with the generic flight inlet.

Figure 2 (b) and Figure 4 (b) shows the Mach and pressure distribution on the center plane for the non-distorted direct-connect mode. Figure 3 and Figure 5 show that the average Mach and pressure are consistent with the flight inlet from the engine throat through the end of the isolator.

4.1.3 Distorted direct-connect mode

The design of the distortion generator hardware proceeded from the CFD results for the flight inlet. The procedure developed in Reference 1 results in a new facility nozzle that generates the flow properties in region C (see Figure 1), where the flow is parallel to the cowl. For the generic inlet at the matching flight condition, the Mach number in region C is approximately 2.50, and the shock that separates region C from region D is generated 94 mm upstream of the engine throat. That location defines the start of the compression region of the distortion generation device. A method-of-characteristic procedure with boundary layer corrections was used to define a nozzle that provides the Mach 2.50 conditions. Figure 6 shows a schematic of the distortion generator configuration. The facility nozzle that generates Mach 2.50 flow and the compression section from the shock reflection point 94 mm upstream of the throat will likely be constructed as a single unit for the planned experimental program.

Figure 2 and Figure 4 show the Mach and pressure distribution on the center plane for the distorted direct-connect mode, and show similar shock structures as the flight inlet. Figure 3 and Figure 5 show that the average Mach and pressure are consistent with the flight inlet from the shock reflection point 94 mm upstream of the engine throat through the end of the isolator.

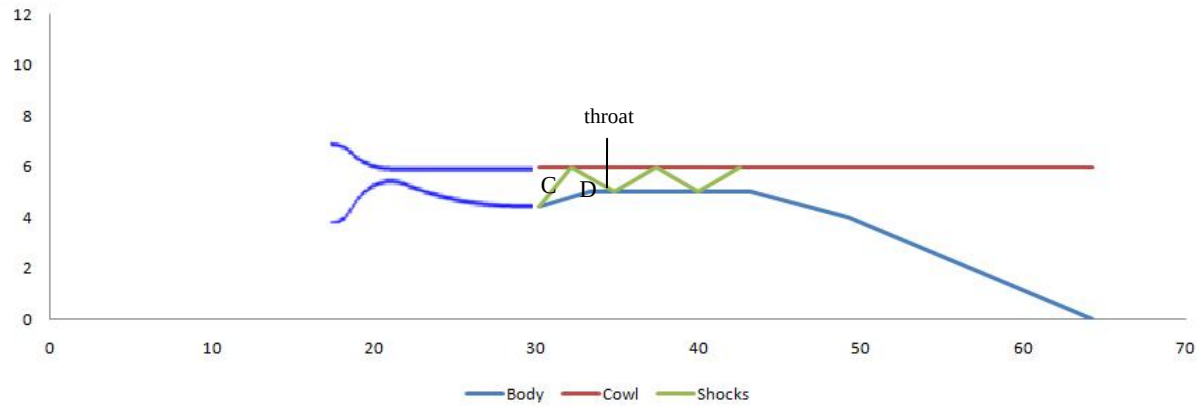

Figure 6: Schematic of distortion generator configuration

Comparisons of body and cowl centerline wall pressure of the three testing modes are included in Figure 7 and Figure 8. Excellent agreement between the flight and distorted direct-connect modes is seen, showing a similar oscillating pressure caused by the reflections of the inlet shock and shoulder expansion. As expected, the non-distorted direct-connect pressures show a smoothly increasing pressure caused by the supersonic deceleration of the flow due to wall friction.

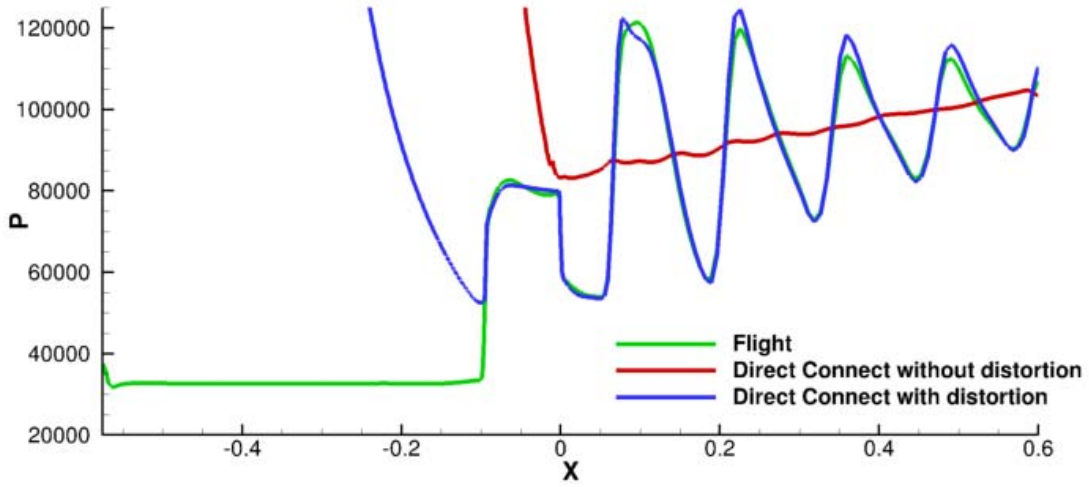

Figure 7: Body side centerline wall pressure comparison

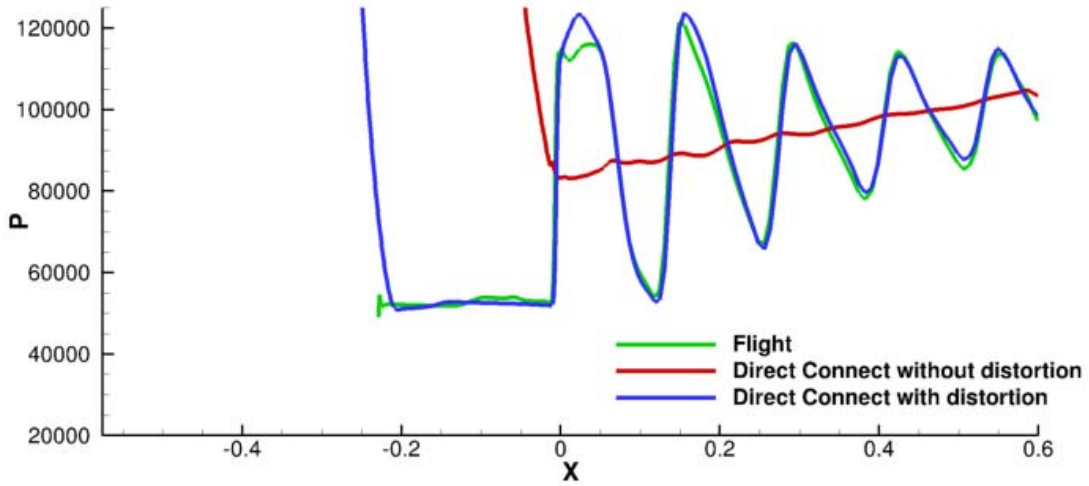

Figure 8: Cowl-side centerline pressure comparison

The preceding data shows how well the distorted direct-connect mode matches the average conditions and shock structure of the flight mode. However, models such as Equation 1 also relate isolator performance to boundary layer parameters such as momentum thickness. Computations of momentum thickness on the centerline are shown in The direct-connect without distortion mode is seen to have thinner boundary layers than the flight, while the direct-connect with distortion has values closer to the flight values.

Mode	**θ (body)**	**θ (cowl)**
Flight	0.638 mm	0.476 mm
Direct-Connect without distortion	0.226 mm	0.226 mm
Direct-Connect with distortion	0.512 mm	0.693 mm

Table 1: Momentum thickness on centerline at engine throat

However, the computation of the momentum thickness has some ambiguity for internal distorted flows due to an ill-defined edge condition. Another approach to comparing boundary layer parameters is to compare wall shear stress. Comparisons of the wall shear stress on the body and cowl centerlines are shown in Figure 9 and Figure 10. It is seen that the distorted direct-connect mode more closely matches the wall shear stress expected in flight, in agreement with the momentum thickness results.

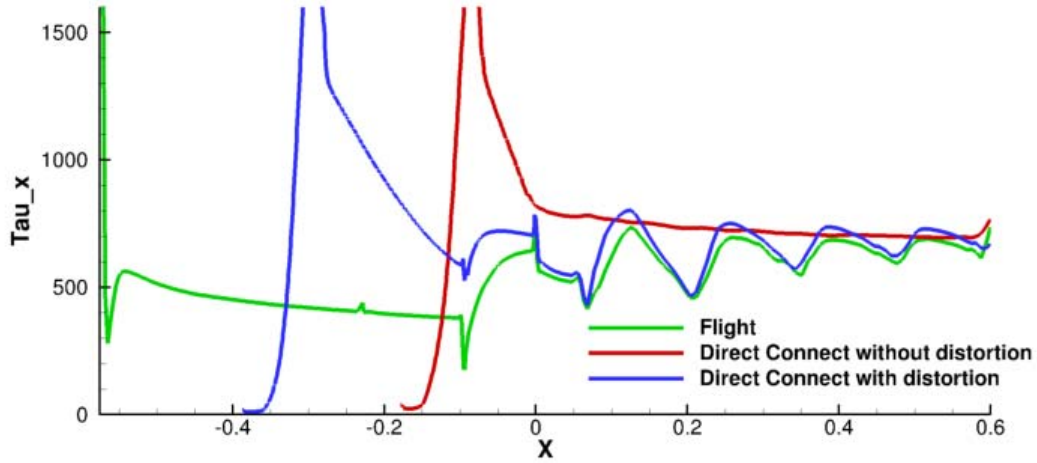

Figure 9: Body-side centerline shear stress comparison

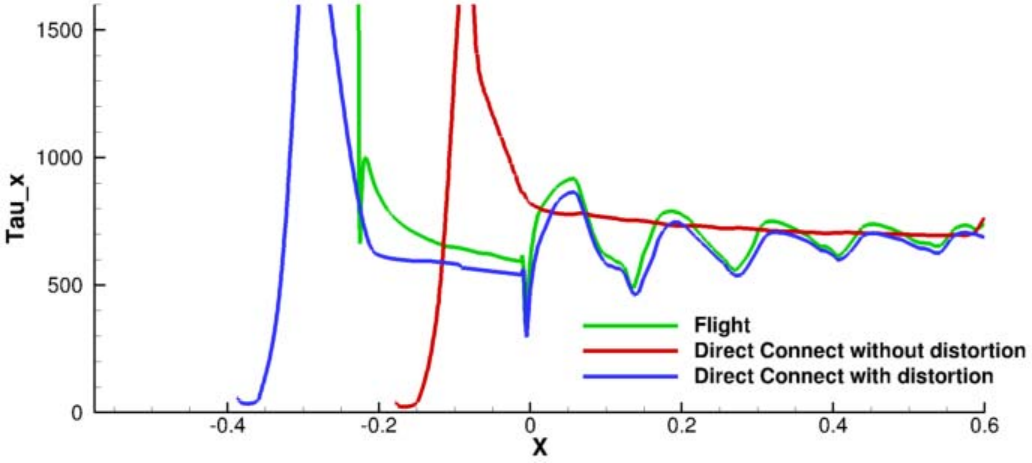

Figure 10: Cowl-side centerline shear stress comparison

Figure 11 shows Mach number in a plane just downstream of the throat. The direct-connect with distortion mode is seen to capture the general shape of the flow distortion that is seen in flight. Note, however, that the corner boundary layers on the cowl side are much thicker in the distorted direct-connect mode than in flight. A closer look at the profiles on the centerline at the same plane is shown in Figure 12. The slope of the Mach profiles at the wall indicates that the wall shear is similar for the distortion mode and the flight mode, but the overall boundary layer thickness and shape are still somewhat different. For completeness, Figure 13 shows that the pressure profiles at the engine throat are well represented in the distortion case.

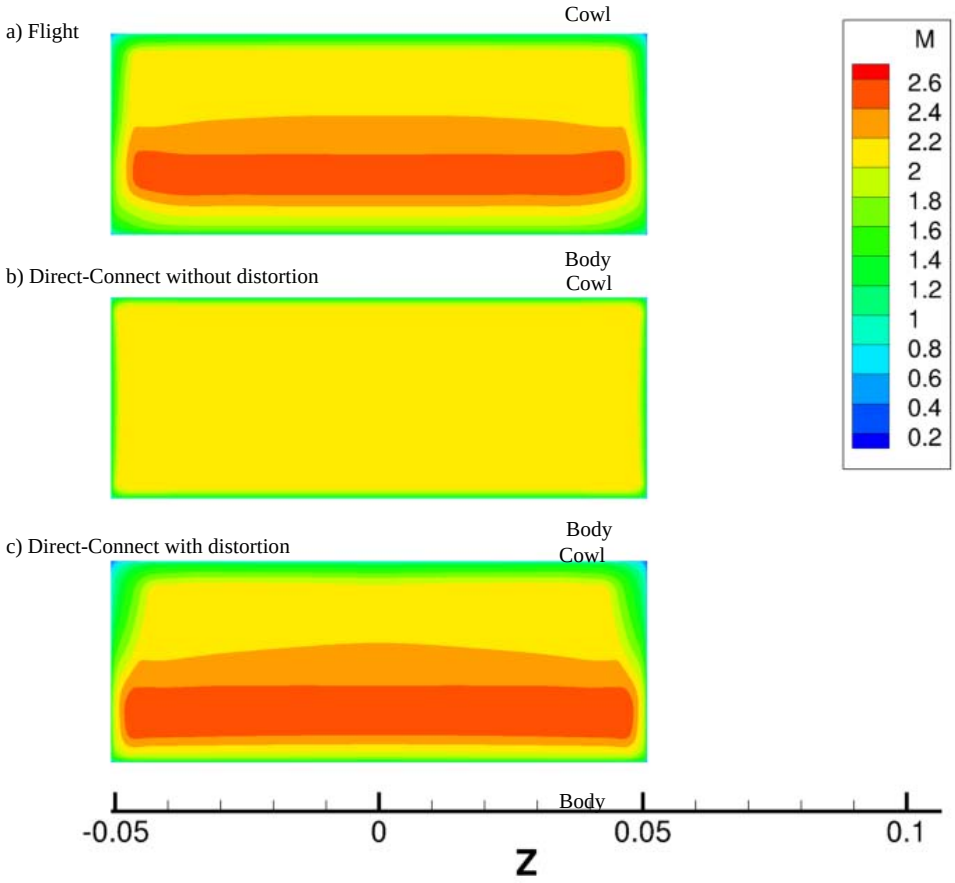

Figure 11: Mach number distribution in plane just after throat

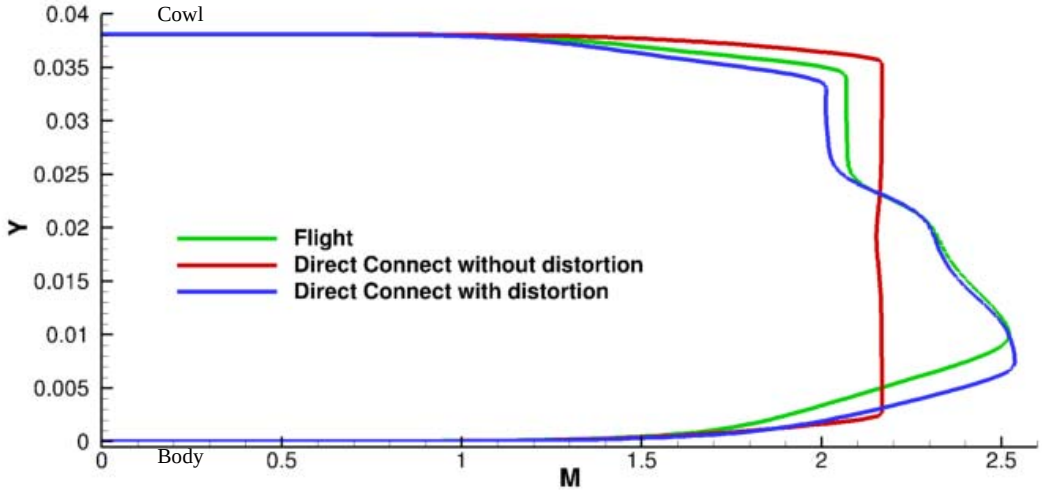

Figure 12: Mach distribution on center plane just after throat

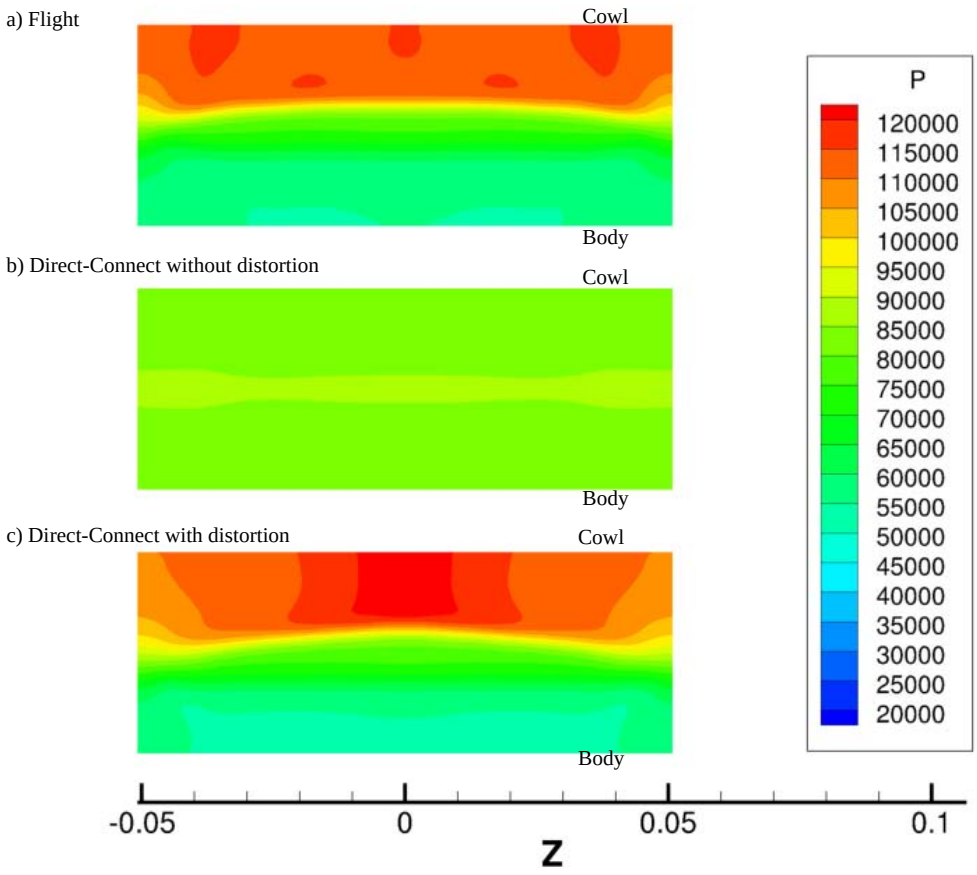

Figure 13: Pressure distribution in plane just after throat

4.2 CFD Analysis of Isolator Performance

The objective of the research project is to gain an understanding of the impact of flow distortion on scramjet performance. The first area to be studied is the effect of flow distortion on the flow phenomena in the isolator. CFD simulations using RANS methodology have been performed for a range of back pressures; however the current paper will focus on RANS simulations for a single back pressure which is representative of the isolator behavior. A companion experimental study is planned which will provide additional information, and hybrid RANS/LES CFD analysis will also be performed.

The average throat pressure for all three modes is approximately 82 kPa, and the results presented here utilized an exit pressure of 340 kPa, for a pressure ratio of 4.1. The normal shock pressure ratio for the inflow Mach number of 2.18 is 5.38, so the current case represents 77% of the theoretical maximum pressure rise. The isolator length is 600 mm, which is 15.7 times the height, and should provide adequate length for a complete shock train.

Figure 14 shows the average pressures at each streamwise location in the isolator for each of the three testing modes, normalized by the pressure at the start of the shock train, which is approximately 88 kPa in each case. The pressure ratio between the exit BC and the start of the shock train is 3.86. No significant change is shock position is seen, despite the significant difference in the incoming profiles as discussed above. This figure also shows the shock rise predicted by the Sullins model (Equation 1) for each case. The Sullins isolator model and the CFD results show a reduced pressure gradient in the early part of the shock train for the distorted direct-connect and flight cases, consistent with the thicker boundary layers in these cases. However, the CFD shows that the distance required to reach a pressure ratio of 3.5 is equal for all three cases, contrary to the Sullins model. Figure 15 and Figure 16 show the Mach and pressure distribution on the isolator center plane, and no significant change in shock position is

observable. Figure 17 shows the mass flux distribution in the center plane for the three configurations. At high back pressure, the flight and distorted direct-connect modes show a significant shift of the mass flux to the cowl surface, while the mass flux remains centered in the undistorted direct-connect mode. This shift of mass flux toward one all has implications on scramjet fueling, that might indicate that conventional direct-connect testing might not capture. More studies are planned in this area.

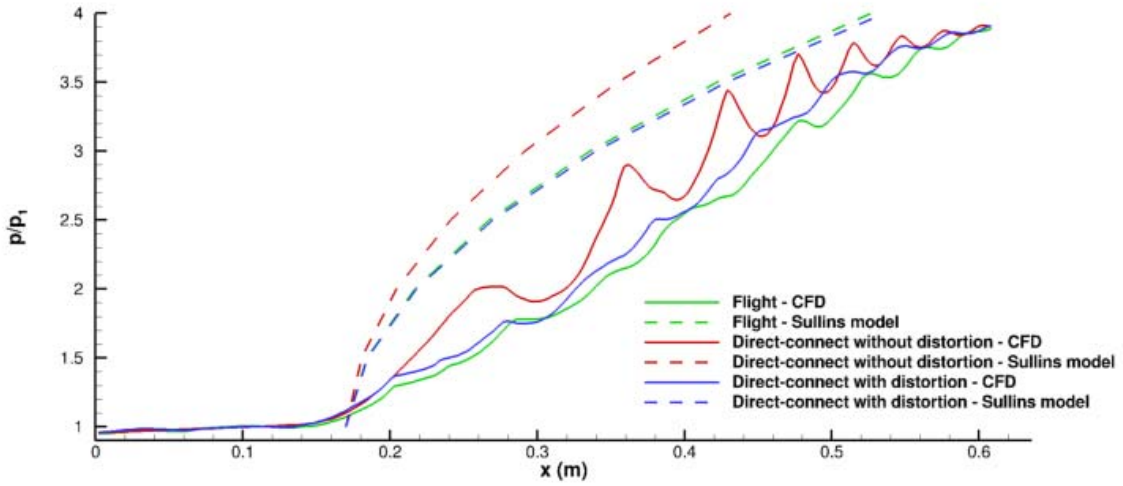

Figure 14: Isolator pressure rise for exit pressure of 340 kPa

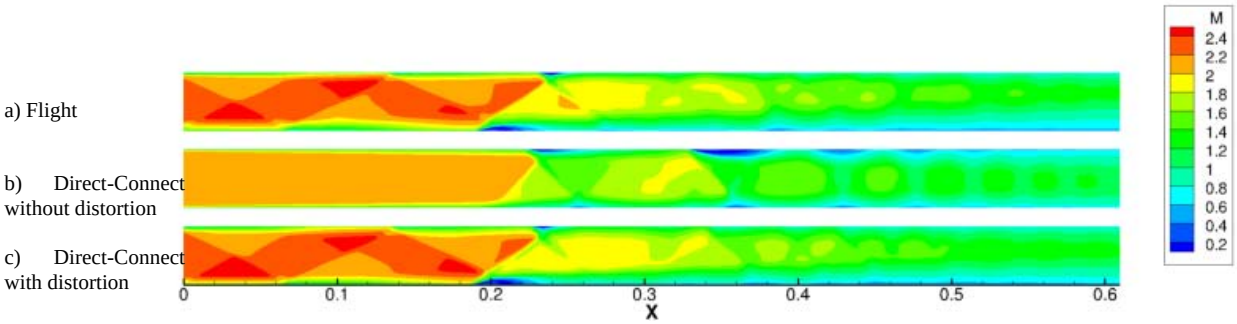

Figure 15: Isolator center plane Mach distribution for exit pressure of 340 kPa

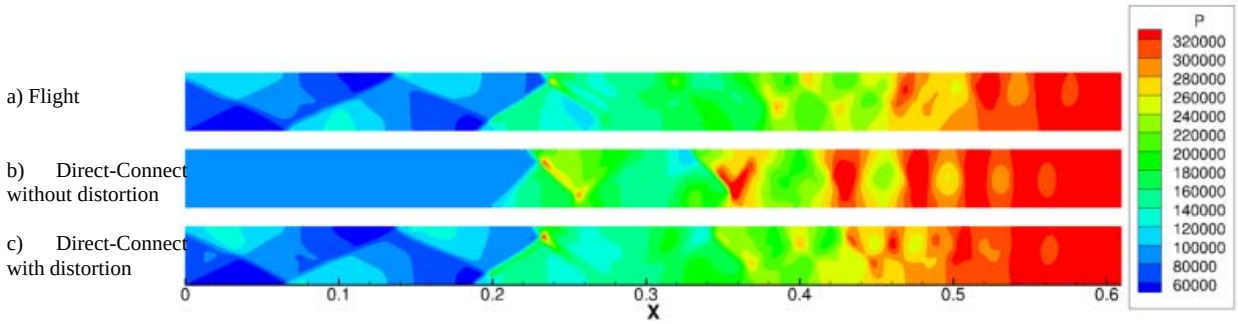

Figure 16: Isolator center plane pressure distribution for exit pressure of 340 kPa

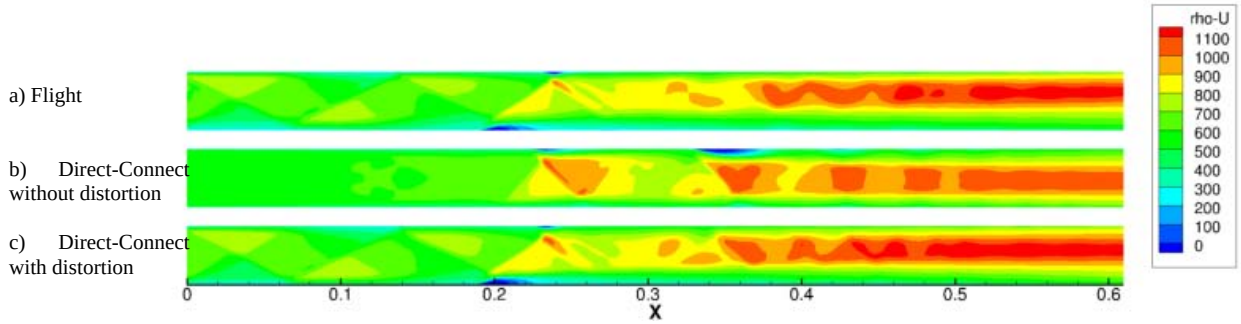

Figure 17: Isolator center plane mass flux distribution for exit pressure of 340 kPa

5.0 Conclusions and Recommendations

An approach to simulate the flow distortion caused by inlet compression has been demonstrated for a direct- connect test facility. The objective is to study the impact of this flow distortion on scramjet performance. The first CFD study of this distortion generation approach indicates that no change in isolator shock position should be expected. However, differences were observed in the rate of pressure rise within the shock train, and in the mass flux distribution at the exit plane of the isolator. More detailed CFD studies using hybrid RANS/LES approaches are planned, as well as an experimental study in an AFRL/RZA direct-connect facility. Future studies include examination of the impact of inflow distortion on injection and mixing.

6.0 Acknowledgments

The authors appreciate the support given by the Air Force Office of Scientific Research under program manager Dr. Julian Tishkoff. The authors gratefully acknowledge the computational resources provided by the DoD High Performance Computing Modernization Program, and the support of the staff at the AFRL and ARL DoD Supercomputing Resource Centers.

7.0 References

1. Gruber, M. R., Hagenmaier, M. A., and Mathur, T., “Simulating Inlet Distortion Effects in a Direct-Connect Scramjet Combustor”, AIAA 2006-4680, 2006.

2. CFD++ User Manual, Metacomp Technologies Inc, http://www.metacomptech.com, 2010,

3. Gridgen User Manual, Pointwise Inc, http://www.pointwise.com, 2010,

4. Hagenmaier, M., and Davis, D. “Scramjet Component Optimization using CFD and Design of Experiments,” AIAA-2002-0544, 2002.

5. Gruber, M. R., Barhorst, T., et. al, “Instrumentation and Performance Analysis Plans for the HIFiRE Flight 2 Experiment”, AIAA 2009-5032, 2009.

6. Sullins, G., and McLafferty, G., “Experimental Results of Shock Trains in Rectangular Ducts”, AIAA-92-5103, 1992.